

# A chromosome-level genome assembly for *Dracaena cochinchinensis* reveals the molecular basis of its longevity and formation of dragon's blood

Yanhong Xu<sup>1,6</sup>, Kaijian Zhang<sup>4,6</sup>, Zhonglian Zhang<sup>3,6</sup>, Yang Liu<sup>1,6</sup>, Feifei Lv<sup>2</sup>, Peiwen Sun<sup>1</sup>, Shixi Gao<sup>1</sup>, Qiuling Wang<sup>1</sup>, Cuicui Yu<sup>1</sup>, Jiemei Jiang<sup>1</sup>, Chuangjun Li<sup>5</sup>, Meifang Song<sup>3</sup>, Zihui Gao<sup>1</sup>, Chun Sui<sup>1</sup>, Haitao Li<sup>3</sup>, Yue Jin<sup>1</sup>, Xinwei Guo<sup>1</sup> and Jianhe Wei<sup>1,2,\*</sup>

<sup>1</sup>Key Laboratory of Bioactive Substances and Resources Utilization of Chinese Herbal Medicine, Ministry of Education & National Engineering Laboratory for Breeding of Endangered Medicinal Materials, Institute of Medicinal Plant Development, Chinese Academy of Medical Sciences and Peking Union Medical College, Beijing 100193, China

<sup>2</sup>Hainan Branch of the Institute of Medicinal Plant Development, Chinese Academy of Medical Sciences and Peking Union Medical College, Haikou 570311, China

<sup>3</sup>Yunnan Key Laboratory of Southern Medicine Utilization, Yunnan Branch of the Institute of Medicinal Plant Development, Chinese Academy of Medical Sciences and Peking Union Medical College, Jinghong 666100, China

<sup>4</sup>Novogene Bioinformatics Institute, Beijing 100083, China

<sup>5</sup>Institute of Materia Medica, Chinese Academy of Medical Sciences and Peking Union Medical College, Beijing 100050, China

<sup>6</sup>These authors contributed equally to this article.

\*Correspondence: Jianhe Wei ([wjianh@263.net](mailto:wjianh@263.net))

<https://doi.org/10.1016/j.xplc.2022.100456>

## ABSTRACT

*Dracaena*, a remarkably long-lived and slowly maturing species of plant, is world famous for its ability to produce dragon's blood, a precious traditional medicine used by different cultures since ancient times. However, there is no detailed and high-quality genome available for this species at present; thus, the molecular mechanisms that underlie its important traits are largely unknown. These factors seriously limit the protection and regeneration of this rare and endangered plant resource. Here, we sequenced and assembled the genome of *Dracaena cochinchinensis* at the chromosome level. The *D. cochinchinensis* genome covers 1.21 Gb with a scaffold N50 of 50.06 Mb and encodes 31 619 predicted protein-coding genes. Analysis showed that *D. cochinchinensis* has undergone two whole-genome duplications and two bursts of long terminal repeat insertions. The expansion of two gene classes, *cis*-zeatin O-glucosyltransferase and small auxin upregulated RNA, were found to account for its longevity and slow growth. Two transcription factors (bHLH and MYB) were found to be core regulators of the flavonoid biosynthesis pathway, and reactive oxygen species were identified as the specific signaling molecules responsible for the injury-induced formation of dragon's blood. Our study provides high-quality genomic information relating to *D. cochinchinensis* and significant insight into the molecular mechanisms responsible for its longevity and formation of dragon's blood. These findings will facilitate resource protection and sustainable utilization of *Dracaena*.

**Key words:** genome, *Dracaena cochinchinensis*, dragon's blood, longevity, flavonoid biosynthesis, ROS

Xu Y., Zhang K., Zhang Z., Liu Y., Lv F., Sun P., Gao S., Wang Q., Yu C., Jiang J., Li C., Song M., Gao Z., Sui C., Li H., Jin Y., Guo X., and Wei J. (2022). A chromosome-level genome assembly for *Dracaena cochinchinensis* reveals the molecular basis of its longevity and formation of dragon's blood. *Plant Comm.* **3**, 100456.

## INTRODUCTION

Dragon's blood, the red resin produced by tree species in the genus *Dracaena* (Asparagaceae), is a precious traditional Chi-

Published by the Plant Communications Shanghai Editorial Office in association with Cell Press, an imprint of Elsevier Inc., on behalf of CSPB and CEMPS, CAS.

nese medicine and a folk medicine used by many nationalities across the world. It has several therapeutic functions and can activate blood circulation, dissipate blood stasis, relieve inflammation and pain, and improve astringency and hemostasis (Gupta et al., 2008; Fan et al., 2014; Sun et al., 2019). Apart from being a famous medicine, dragon's blood is also used as a colorant for artwork in many cultures (Zheng et al., 2012). It is called dragon's blood because the resin or sap excreted by some members of the genus *Dracaena* after external injury or microbial invasion is deep red in color and looks like the blood of a legendary dragon (Gupta et al., 2008). Therefore, *Dracaena* has become famous all over the world for its red resin and belongs to the cultural heritage of humanity.

*Dracaena* species are monocotyledonous evergreen plants that are mainly distributed in tropical and subtropical regions of Asia and Africa. These are remarkably long-lived and slow-growing species and are renowned for their longevity (Zheng et al., 2012; Tomlinson and Huggett, 2012; Maděra et al., 2018, 2020). The age of a famous dragon's blood tree was previously estimated to be several thousands of years (Humboldt, 1814; Christ, 1886; Schenck, 1907). However, subsequent analysis of several of the largest trees concluded that their age was more likely to be several hundred years and that the flowering period varies from 10 years to several decades (Pütter, 1925; Symon, 1974; Mägdefrau, 1975; Zheng et al., 2012; Maděra et al., 2018). According to previous research, the juvenile stages of *D. cinnabari* from seedling to first flowering can take 200–250 years or even more (Maděra et al., 2018), thus demonstrating that this species takes an extremely long time to grow and mature. Owing to difficulties related to investigating natural population aging, several methodologies have been developed for age estimation in such trees (Adolt and Pavliš, 2004; Adolt et al., 2012; Jura-Morawiec, 2019; Lengálová et al., 2020). These methods have all demonstrated that the dragon tree is a long-lived species.

There is much confusion surrounding the origin and identity of dragon's blood trees, and many plants can produce dragon's blood, including *Croton*, *Dracaena*, *Daemonorops*, and *Pterocarpus* (Gupta et al., 2008; Ding et al., 2020). In the wild, *Dracaena* grows slowly, and only trees that are over 30 years of age have been shown to produce dragon's blood (Edwards et al., 1997; Wang et al., 2013; Ding et al., 2020). Due to continuous over-exploitation, *Dracaena* are now threatened with depletion. In 1998, many *Dracaena* species were listed on the International Union for Conservation of Nature Red List (IUCN Red List, 2017.2). Of these, *Dracaena cochinchinensis* and *D. cambodiana* were rated as vulnerable in China (Hubáľková et al., 2015; Kamel et al., 2018). Soon afterward, these two species were placed on the List of National Key Protected Wild Plants of China; this represents the second highest grade of national protection, and the felling of such endangered species is prohibited. Because of the endangered status of *D. cochinchinensis* and the fact that it is now a limited genetic resource, it is critical to consider adequate measures for its conservation management and to protect against its exploitation.

In China, *D. cochinchinensis* is the official original species found to produce dragon's blood (Zheng et al., 2009; Luo et al., 2011) and was first discovered by Xitao Cai in 1972 in Yunnan

province. This species is commonly used as a substitute for the traditionally imported dragon's blood, called Long-Xue-Jie (Chinese dragon's blood). According to literature surveys, dragon's blood has been recorded and used medicinally in China for at least 1500 years. The authentic source of ancient Chinese *Dracaena* was thought to have been imported from Africa (Cai and Xu, 1979). With increased levels of shipping, the genuine form of *Dracaena* changed from the resin of *Dracaena* in the agave family to the red resin of the rattan fruit in Southeast Asia until the discovery of *D. cochinchinensis*, which is exclusively found in China (Cai and Xu, 1979; Zheng et al., 2006; Wang et al., 2011).

Flavonoids are the main components of dragon's blood. Flavonoid oligomers, composed of one dihydrochalcone unit condensed with one or more chalcone, flavane, or homoisoflavane units, constituted the major identified components of dragon's blood from the genus *Dracaena* (Pang et al., 2016). Oligomeric flavonoids account for over 50% of the resin produced by *Dracaena* spp. by weight (Hao et al., 2015). Thus far, hundreds of flavonoids have been isolated from the resin wood of *D. cochinchinensis* (for reviews, see Gupta et al., 2008; Fan et al., 2014; Sun et al., 2019). In addition, terpenoids and steroidal saponins are also effective components of dragon's blood (Fan et al., 2014; Teng et al., 2015; Maděra et al., 2020; Vanickova et al., 2020); these components have been reported to be cytotoxic and could be used as anticarcinogens (Darias et al., 1989; Mimaki et al., 1999; González et al., 2003; Hernández et al., 2004; Ding et al., 2020; Maděra et al., 2020).

Although many previous studies have described the chemical constituents and pharmacological effects of dragon's blood (for reviews, see Gupta et al., 2008; Fan et al., 2014; Sun et al., 2019; Maděra et al., 2020), little is known about the molecular mechanisms responsible for its formation. In this study, we report the draft genome sequence of *D. cochinchinensis* at the chromosome level. We also conducted transcriptomic and metabolomic analysis. Our findings represent an important resource that can enhance our understanding of the fundamental biology and molecular basis of *D. cochinchinensis*, thus providing a foundation from which to generate new conservation management strategies.

## RESULTS

### Genome sequencing, assembly, and annotation

A genome survey using k-mer analysis ( $k = 17$ ) revealed that the size of the *D. cochinchinensis* genome was approximately 1.257 Gb with a heterozygosity of 0.52% and a repeat sequence ratio of 67.8% (Supplemental Figure 1; Supplemental Table 1). Based on the estimated genome size, using a combination of SMART sequencing technology from PacBio, along with 10x Genomics and short-read sequencing from Illumina platforms, we obtained a total of 407.06 Gb of clean data, thus representing 323.75× coverage (Supplemental Table 2). The initial assembly was 1.21 Gb in size, containing 1898 scaffolds and 3042 contigs, with a scaffold N50 size of 2.07 Mb and a contig N50 size of 1.1 Mb (Supplemental Table 3). Assessment of the completeness of the genome assembly with CEGMA indicated 96.77% coverage of the conserved core eukaryotic genes, and Benchmarking Universal

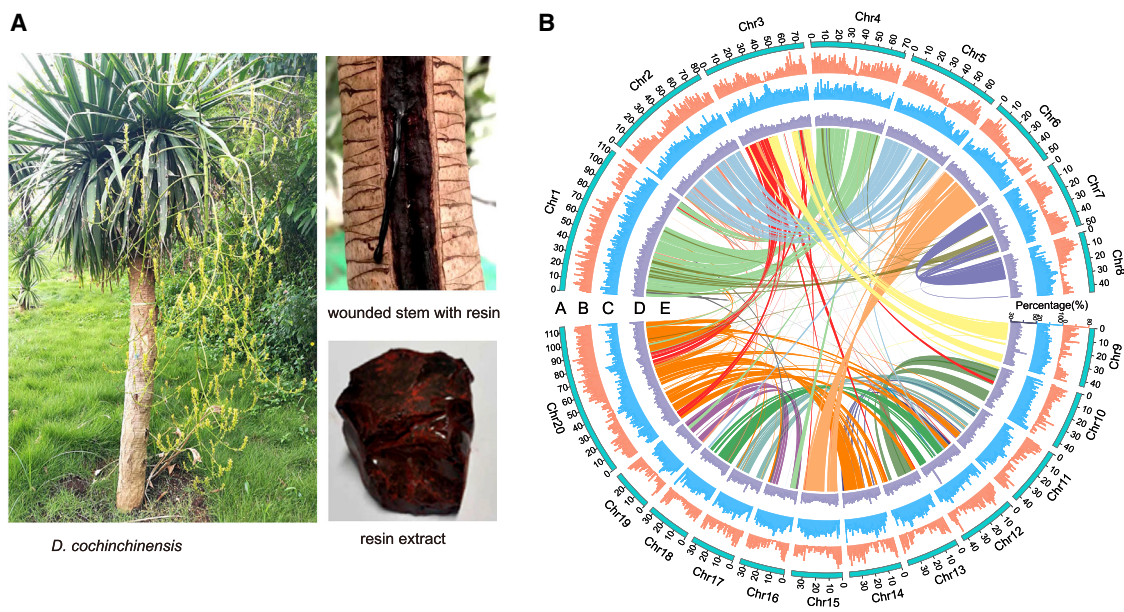


**Figure 1. Morphological and genomic features of *D. cochinchinensis*.**

**(A)** Morphology of *D. cochinchinensis* and dragon's blood.

**(B)** Overview of the *D. cochinchinensis* draft genome assembly. **(a)** The 20 chromosomes of *D. cochinchinensis*, with a resolution of 5 Mb. **(b)** Gene density, with a sliding window of 500 kb. **(c)** Percentage of repeats, with a sliding window of 500 kb. **(d)** GC content, with a sliding window of 100 kb. **(e)** Each linking line in the center of the circle connects a pair of homologous genes.

Single-Copy Ortholog analyses (Simao et al., 2015) showed that the genome was 93.6% complete (Supplemental Table 4). These results suggested that the genome assembly was relatively complete and of high quality. Next, approximately 137.26 Gb of high-quality Hi-C data were used to further improve the genome assembly, and 90.26% of the genome was anchored onto 20 chromosomes ( $2n = 40$ ) (Figure 1B; Supplemental Figures 2 and 3; Supplemental Table 5). The final assembly consisted of 1835 scaffolds, spanning 1.21 Gb, with a scaffold N50 size of 50.05 Mb (Supplemental Table 6).

Based on *de novo* and homology-based predictions and transcriptome data, a total of 31 619 protein-coding genes were predicted, and 31 402 genes (99.3%) were assigned specific functions (Supplemental Table 7). In addition, by comparing with the known noncoding RNA libraries, we obtained noncoding RNA information relating to the *D. cochinchinensis* genome (Supplemental Table 8), including 1570 transfer RNAs, 1278 ribosomal RNAs, 1576 microRNAs, and 722 small nuclear RNAs.

### Genomic evolution of *D. cochinchinensis*

*D. cochinchinensis* belongs to the Asparagales clade of monocotyledons and is close to *Asparagus officinalis*, *Dendrobium officinale*, and *Apostasia shenzhenica*, which have completed genome sequences. We clustered the annotated genes into gene families among these species along with additional monocot and dicot species, including *A. officinalis*, *D. officinale*, *A. shenzhenica*, *Elaeis guineensis*, *Oryza sativa*, *Ananas comosus*, *Musa acuminata*, *Arabidopsis thaliana*, *Populus trichocarpa*, *Aquilaria sinensis*, *Hevea brasiliensis*, *Citrus grandis*, *Carica papaya*, *Eucalyptus grandis*, *Vitis vinifera*, and *Amborella trichopoda*. Family clustering yielded 31 324 gene families (groups), including 252

single-copy families. Evolutionary trees were constructed based on coding sequences using RAxML software. *D. cochinchinensis* and *A. officinalis* were gathered in one branch, as were *D. officinale* and *A. shenzhenica*, thus indicating that *Asparaginaceae* and *Orchidaceae* underwent independent divergence long ago (138.4 Mya); the time of divergence between *D. cochinchinensis* and *A. officinalis* was 87.7 Mya (Figure 2A).

To investigate the genome expansion in *D. cochinchinensis*, we analyzed whole-genome duplication (WGD) events. Four-fold degenerate site (4DTV) values were estimated based on paralogous gene pairs in collinear regions detected in *D. cochinchinensis* and three other representative plant species (*A. officinalis*, *D. officinale*, and *A. shenzhenica*). The distribution of 4DTV distances in *D. cochinchinensis* showed two peaks at approximately 0.12 and 0.45 (Figure 2B). The first peak shared by *D. cochinchinensis* and *A. officinalis* may correspond to the Asparagales- $\beta$  event previously identified in the *A. officinalis* genome (Harkess et al., 2017; Li et al., 2020). The second peak at approximately 0.12 indicated that *D. cochinchinensis* underwent another WGD event independently after diverging from *A. officinalis* (Figure 2B and Supplemental Figure 4). To further confirm that *D. cochinchinensis* had undergone two WGD events, we detected syntenic blocks across the *D. cochinchinensis* genome and the *A. trichopoda* genome and performed synteny analysis. We found that *D. cochinchinensis* had experienced the Asparagales- $\beta$  event and another WGD event, as suggested by the 4:1 syntenic relationship between *D. cochinchinensis* and *A. trichopoda* (Supplemental Figure 5). Our analysis thus provides convincing evidence for two rounds of whole-genome diploidization events in the *D. cochinchinensis* genome. In total, 29 280 duplicated genes were identified and classified into five categories: 6864 WGDs (23.1%), 1506 tandem duplicates

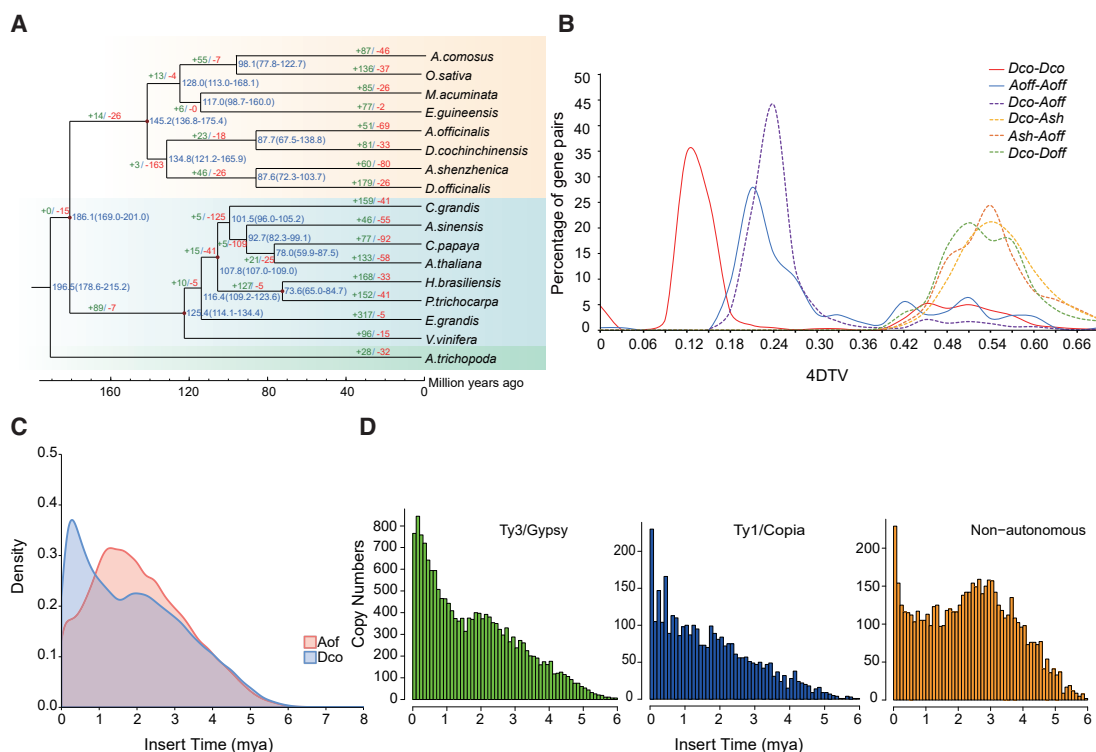


**Figure 2. Comparative genomic analysis.**

**(A)** Phylogenetic tree of 17 plant species. Divergence time (Mya) estimates are indicated by the blue numbers beside the branch nodes. The numbers of gene-family contractions and expansions are indicated by green and red numbers, respectively.

**(B)** Distribution of 4DTV for paralogous genes among *D. cochinchinensis*, *A. officinalis*, *D. officinale*, and *A. shenzhenica*.

**(C)** Estimation of LTR activity showed two insertion burst events in the *D. cochinchinensis* genome (Mya).

**(D)** In the recent burst of activity, most of the elements responsible were autonomous (3359 copies of Ty1-copia and 16 897 copies of Ty3-gypsy) and non-autonomous LTRs (5861 copies) with peaks of activity <6 Mya.

(5.1%), 1196 proximal duplicates (4.1%), 7301 transposed duplicates (24.9%), and 19 613 dispersed duplicates (66.7%). Next, we investigated the duplications of genes involved in flavonoid biosynthesis (i.e., *PAL*, *4CL*, *C4H*, *CHI*, *CHS*, *DFR*, *F3H*, *FLS*, *FAR*, *PPO*, and *OMT*) and found that some genes were duplicated in a different manner. Some genes were retained after WGD, thus suggesting that the recent WGD event played an important role in the evolution of flavonoid biosynthesis in *D. cochinchinensis* (Supplemental Table 9).

### LTR insertion and genome size expansion

Further analysis showed that 60.15% (729.11 Mb) of the *D. cochinchinensis* genome consists of repetitive sequences (Supplemental Table 10); this is similar to *D. officinale* (63.33%) (Yan et al., 2015) and *E. guineensis* (57%) (Singh et al., 2013) but higher than *A. shenzhenica* (42.05%) (Zhang et al., 2017a) and *A. comosus* (43.7%) (D'hont et al., 2012). As in many other sequenced plant genomes (Kim et al., 2014; Teh et al., 2017; Zhang et al., 2017b), long terminal repeat retrotransposons (LTR-RTs) dominated, accounting for 51.06% of the assembly; 41% of the genome sequence comprised *Gypsy* elements (501 175 881 bp), and 5.9% comprised *Copia* elements (72 176 608 bp). By analyzing the insertion times of intact LTRs, we found that two insertion bursts had occurred in the *D. cochinchinensis* genome at approximately 0.3–0.4 and 2 million years, respectively (Figure 2C); these events

were dominated by both autonomous and nonautonomous LTRs. Among these, the *Gypsy* family had the largest number of insertions, and there were two obvious insertion peaks (Figure 2D), thus demonstrating that there is a significant relationship between *Gypsy* expansion and genome expansion. Phylogenetic trees of domains in reverse transcriptase genes from complete RTs were constructed for the *Copia* and *Gypsy* superfamilies in *D. cochinchinensis*, *A. officinalis*, and *A. shenzhenica*. We found that the majority of *Gypsy* elements were species specific in *D. cochinchinensis*, whereas the *Copia* superfamily exhibited a different pattern that consisted of elements from all three species (Supplemental Figure 6).

### Comparative genomics demonstrated the adaptation of *D. cochinchinensis*

Copy numbers of homologous gene families vary greatly among different species, caused by differences in rates of gene gain and loss. Analysis using Computational Analysis of Gene Family Evolution (CAFÉ) (Bie et al., 2006) identified 81 expanded gene families in *D. cochinchinensis* compared with the common ancestor of *D. cochinchinensis* and *A. officinalis* (Figure 2A). A total of 730 and 1088 genes in the expanded families were annotated with Gene Ontology terms and Kyoto Encyclopedia of Genes and Genomes (KEGG) pathways, respectively. Gene Ontology analysis revealed that these expanded orthogroups were related to several metabolic processes (Supplemental Table 11;

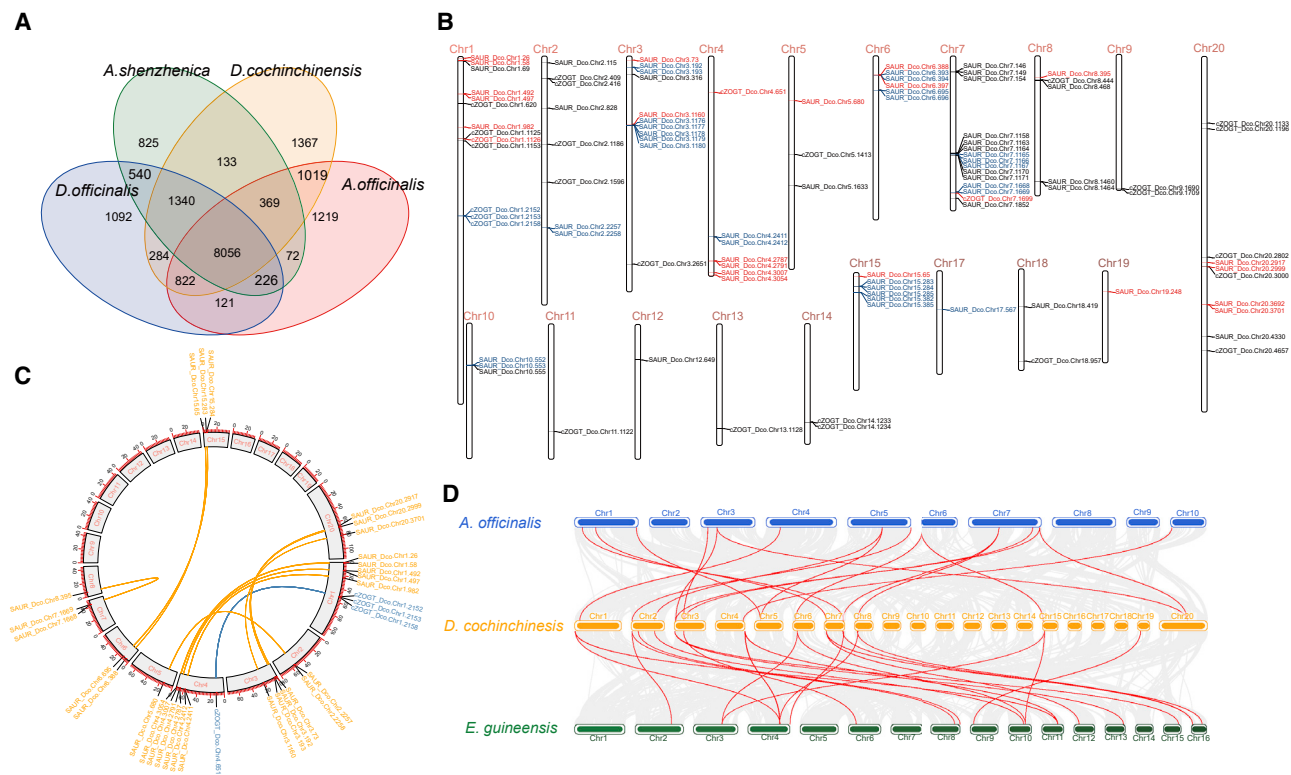


**Figure 3. Expansion of the SAUR and ZOGT gene families.**

(A) Venn diagram showing shared and unique orthologs among the four *Asparagales* species *D. cochinchinensis*, *A. officinalis*, *D. officinale*, and *A. shenzhenica*.

(B) Schematic representation of the *D. cochinchinensis* chromosomes with the positions of the *SAUR* and *ZOGT* genes. The genes marked in blue and red were generated by WGD and tandem duplication events, respectively.

(C) Collinearity of *SAUR* and *ZOGT* genes in *D. cochinchinensis*.

(D) Syntenic analysis of *SAUR* and *ZOGT* genes in *D. cochinchinensis* and two other representative plant species (*A. officinalis* and *E. guineensis*). Paralogous gene pairs from *A. officinalis* and *E. guineensis* were identified in syntenic blocks using JCVI software (v.0.8.4) with a parameter setting of “-cscore = 0.99”. Protein sequences were extracted and viewed in TBtools (v.0.98745).

Supplemental Figures 7 and 8) such as “ATP metabolic process,” and “defense response” in the biological process category and “binding,” “catalytic activity,” “oxidoreductase activity,” and “peroxidase activity” in the molecular function category. The enriched KEGG categories were “plant-pathogen interaction,” “phenylpropanoid biosynthesis,” “zeatin biosynthesis,” “sesquiterpene and triterpenoid biosynthesis,” “flavone and flavonol biosynthesis,” and “photosynthesis” (Supplemental Table 12; Supplemental Figure 9). We hypothesize that these expanded genes are closely related in some way to the functional requirements of environmental adaptability in *D. cochinchinensis* and the formation of dragon’s blood.

We found that 28 genes were under positive selection and showed significant enrichment in KEGG terms related to base excision repair, nucleotide excision repair, mismatch repair, and DNA replication (Supplemental Table 13). These include DNA ligase 1 and DNA excision repair protein, which are involved in DNA-repair pathways that play crucial roles in maintaining genomic integrity, particularly in response to exposure to environmental genotoxins, including ultraviolet light and reactive oxygen species that form in response to the harsh rays of the sun (Schuch et al., 2017; Nisa et al., 2019). The response of cells to DNA damage restores the DNA structure to enable

its original function or simply enables the cell to survive the damage.

Next, we identified unique and shared gene families among the four *Asparagales* species. *D. cochinchinensis* shared 8056 families with *A. officinalis*, *D. officinale*, and *A. shenzhenica*, whereas 1367 gene families, containing 2954 genes, appeared to be unique to *D. cochinchinensis* (Figure 3A; Supplemental Tables 14 and 15). Functional annotation revealed that the expansion of two classes of genes, small auxin upregulated RNA (*SAUR*) genes and *cis*-zeatin O-glucosyltransferase (*cZOGT*) genes, which play a role in zeatin biosynthesis, may be closely related to the slow growth and longevity of *D. cochinchinensis* (Figure 3B and 3C; Supplemental Tables 16 and 17). Interestingly, analysis of the *D. cochinchinensis* genome identified evolutionary gene family expansions of the *SAUR* genes (77 in *D. cochinchinensis*, 27 in *A. officinalis*, 20 in *A. shenzhenica*, 33 in *D. officinale*, 56 in *O. sativa*, and 42 in *E. guineensis*). *SAUR* is an auxin-responsive protein that acts as the plant’s toolbox for the adaptation of growth and development (Ren and Gray, 2015; Stortenbeker and Beme, 2019). Previous studies in rice confirmed that *SAUR* inhibits growth by negatively regulating auxin synthesis and transport. In addition, *SAUR* has been shown to significantly increase anthocyanin content and ABA levels (Kant et al., 2009).

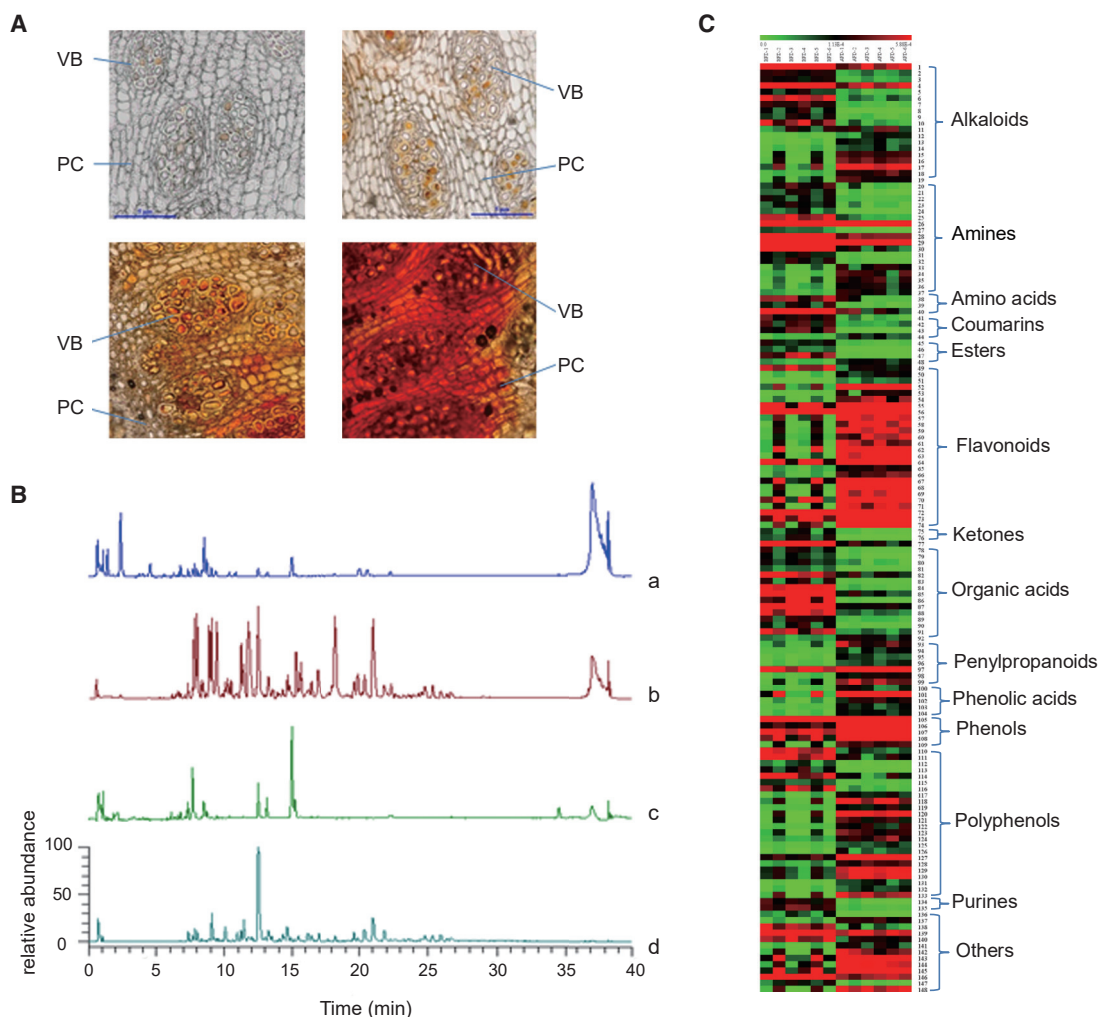


**Figure 4. Histological and metabolic profiling during the formation of dragon's blood.**

(A) Histological images during the formation of dragon's blood in *D. cochinchinensis* (the yellow and red substances in the image are dragon's blood resin). VB, vascular bundle; PC, parenchymal cell. Scale bar: 5  $\mu$ m.

(B) Typical total ion chromatograms of *D. cochinchinensis* (a: positive total ion chromatogram [TIC] before dragon's blood formation; b: positive TIC after dragon's blood formation; c: negative TIC before dragon's blood formation; d: negative TIC after dragon's blood formation).

(C) Heatmap of identified metabolites from *D. cochinchinensis* before and after the formation of dragon's blood (BFD, 1–6 represent six replicates of the analytical materials before the formation of dragon's blood; AFD, 1–6 represent six replicates of the analytical materials after the formation of dragon's blood).

Phylogenetic analysis of SAUR proteins from *D. cochinchinensis* and other species identified 11 subgroups (Supplemental Figure 10). To investigate the potential mechanisms by which SAURs may have expanded, we compared SAUR-containing genomic regions in *D. cochinchinensis* with those of *A. officinalis* and *E. guineensis*. The two species showed strong synteny to *D. cochinchinensis* (Figure 3D). In addition to the SAURs, *cZOGT* had also undergone unique expansion in *D. cochinchinensis* (34 in *D. cochinchinensis*, 0 in *A. officinalis*, 0 in *A. shenzhenica*, 0 in *D. officinale*, 5 in *O. sativa*, 2 in *E. guineensis*, and 0 in *A. thaliana*) and is known to play roles in growth retardation and delay of senescence (Rodo et al., 2008; Kudo et al., 2012). Therefore, the expansion of SAURs and *cZOGT*s is predicted to account for the slow growth and longevity of *D. cochinchinensis*, at least in part, and even its adaptation to the arid environment of karst landforms. To investigate the functions of SAUR and *cZOGT*

genes in *D. cochinchinensis*, we examined their expression levels at different time points after injury (Supplemental Figures 11 and 12). We found that the expression levels of the two genes differed, implying that these genes may have other novel functions in *D. cochinchinensis*.

### Metabolic profiling and differential metabolite pathways in the formation of dragon's blood

Dragon's blood does not appear directly after wounding but instead forms over time. By observing tissue sections, we noted that the color of the resin gradually deepened during the formation of dragon's blood; the resin had filled the vascular bundle and the surrounding parenchymal cells after 90 days (Figure 4A). Eventually, the resin appeared in the form of tear-like drops or chips that coated the site of injury (Figure 1A), protecting the plant from

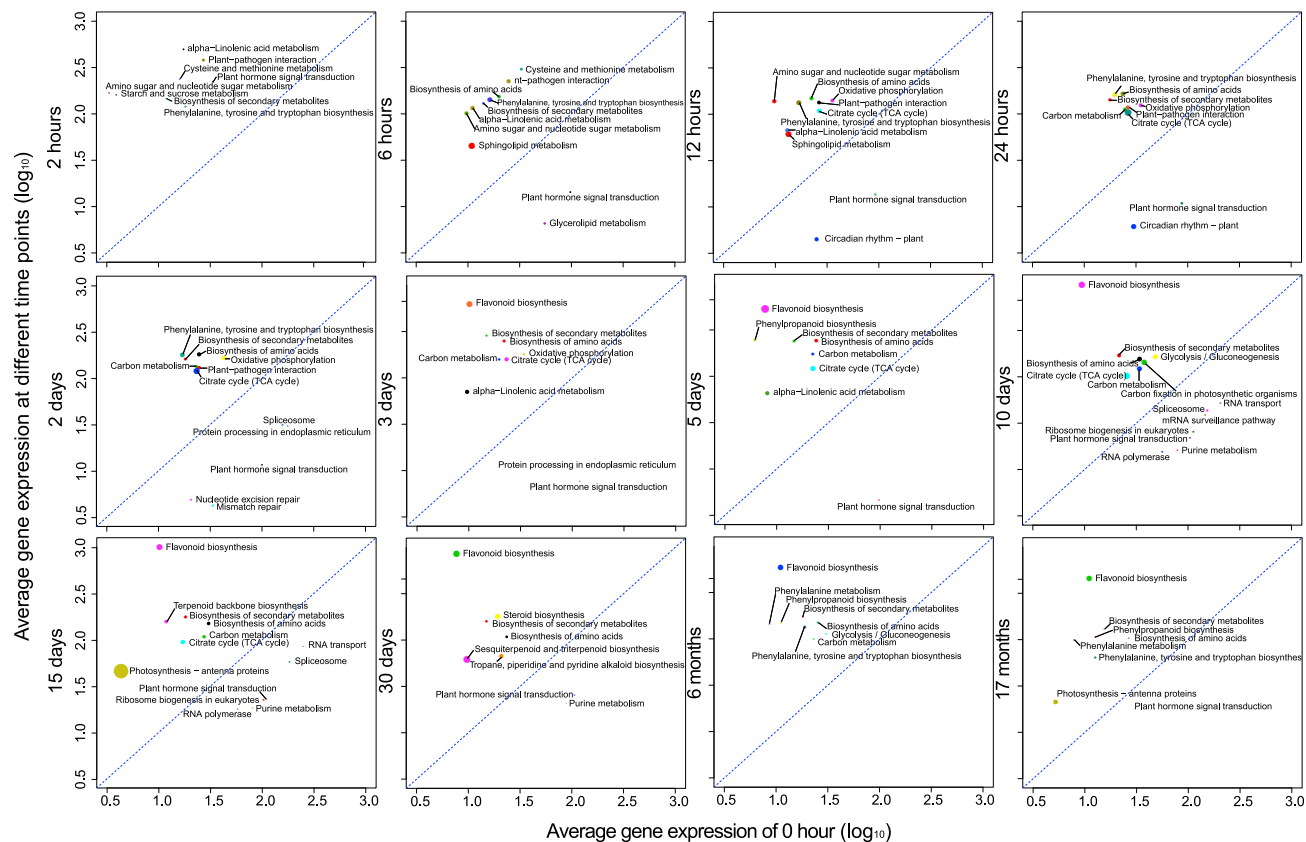


**Figure 5. Differentially expressed metabolic pathways during the formation of dragon's blood.**

Transcriptome analysis identified differentially expressed pathways during the formation of dragon's blood. The upregulated pathways are shown above the oblique line, and the downregulated pathways are below the line. The size of the circles represents the number of genes, and the coordinate value represents the mean times of upregulation or downregulation.

the spread of pathogens. Thus, the formation of dragon's blood is a mechanism by which the tree defends itself (Wang, 2007; Jura et al., 2016; Maděra et al., 2020).

To elucidate the changes in metabolite composition during the formation of dragon's blood, we focused on identifying significant changes in metabolites by filtering selected peaks. Ultimately, a total of 147 differential metabolites were identified or tentatively identified (Supplemental Tables 18 and 19; Figure 4B and 4C). As shown in Figure 4C, the levels of most compounds changed significantly after injury. The levels of 85 compounds increased, including flavonoids, phenols, polyphenols, phenylpropanoids, and phenolic acids, whereas the levels of 62 compounds decreased, including organic acids, amines, and steroids; normalized peak areas showed the same results (Supplemental Figure 13).

Next, we used transcriptomic data to identify the biological processes associated with the formation of dragon's blood. The upregulated differentially expressed genes were mainly enriched in the biological processes "metabolic pathway" and "biosynthesis of secondary metabolites," thus showing that different time points correspond to different metabolic processes (Figure 5). For example, the first metabolic pathways to change (in 2 h) were those related to plant-pathogen interaction and plant hormone signal transduction, as well as starch and sucrose metabolism. Then, the biosynthesis of amino acids and citrate cycle

became significantly enriched; this was followed by flavonoid biosynthesis at 3 days; this lasted for 17 months and represented the most active metabolic pathway. Terpenoid backbone biosynthesis became evident at 15 days, sesquiterpenoid and triterpenoid biosynthesis at 30 days, and phenylpropanoid biosynthesis at 6 months. The differentially expressed metabolic pathways combined with the metabolic profiles are shown in Figure 3C. Our results indicate that the synthesis of dragon's blood involves a series of very complex signal transduction, gene expression regulation, and metabolic processes.

### Genes associated with the biosynthesis of flavonoids in *D. cochinchinensis*

Numerous studies have shown that flavonoids are the main components of dragon's blood (Gupta et al., 2008; Fan et al., 2014) and are associated with the phenylpropanoid biosynthesis pathway (Figure 6). From our genome assembly, we identified 11 gene families related to the formation of dragon's blood (Supplemental Table 20), including some common enzymes in the flavonoid synthesis pathway: PAL, C4H, 4CL, CHS, CHI, F3H, FLS, and DFR. We also identified several downstream biosynthetic genes that produce specific components of dragon's blood. For example, O-methyltransferase forms loureirin A, and polyphenol oxidase forms loureirin B, the index component of standard dragon's blood in China. Gene expression analysis showed that four of the five *CHS* genes and two *CHI* genes were significantly

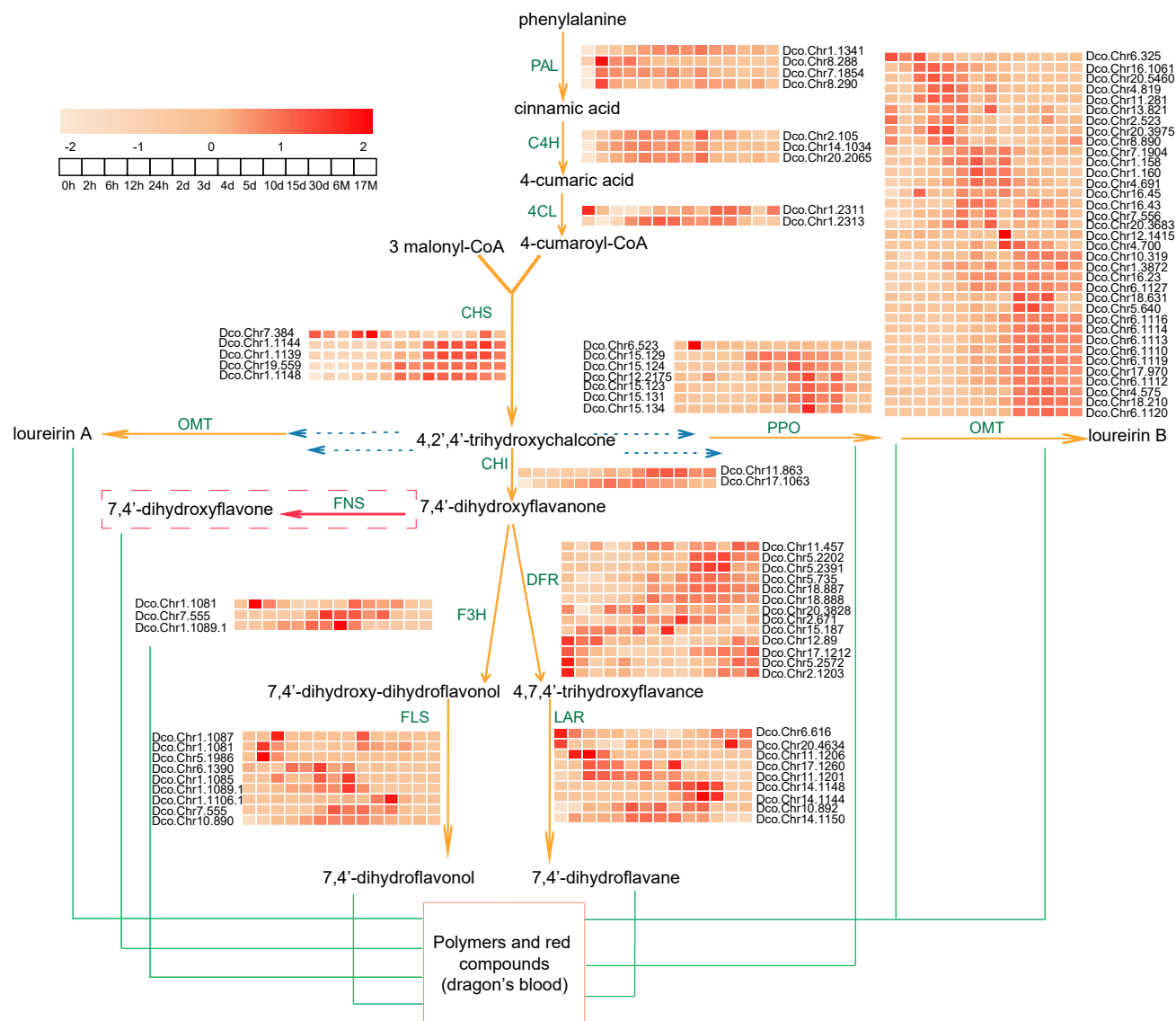


**Figure 6. Flavonoid biosynthesis in *D. cochinchinensis*.**

The flavonoids biosynthesis pathway and the expression profiles (reads per kilobase per million reads mapped) of the genes involved in dragon's blood biosynthesis. PAL, phenylalanine ammonia-lyase; C4H, cinnamate 4-hydroxylase; 4CL, 4-coumarate CoA ligase; CHS, chalcone synthase; CHI, chalcone isomerase; FNS, flavone synthase; F3H, flavanone 3-hydroxylase; DFR, dihydroflavonol 4-reductase; FLS, flavonol synthase; LAR, leucoanthocyanidin reductase; PPO, polyphenol oxidase; OMT: O-methyltransferase.

upregulated after injury; this effect lasted for 17 months. Two of the three *F3H* genes were not expressed in healthy tissues; the highest expression levels occurred 3 and 5 days after injury. Some of the *FLS* and *PPO* members were also expressed at very low levels in healthy stems but were upregulated after injury (Figure 6). We hypothesized that these genes may be specifically involved in the formation of dragon's blood and that their expression is significantly induced by injury.

Furthermore, based on the co-expression model, two types of transcription factors (bHLH and MYB) expressed in wounded stems were predicted to be core regulators of flavonoid synthesis; these transcription factors are likely to target *PAL*, *CHS*, and *FLS* and participate in the regulation of the flavonoid biosynthesis pathway (Supplemental Figure 14; Supplemental Table 21).

Analyzing the 2000 bp upstream of the gene coding region, we found many *cis*-acting elements that were specifically recognized by bHLHs and MYBs (Supplemental Table 22), further demonstrating that these enzyme-encoding genes are likely to be regulated by the two transcription factor types. Moreover, an expression heatmap of *bHLH* and *MYB* genes (Supplemental Figures 15 and 16) showed that they were significantly induced just 2 h after injury. We hypothesize that bHLHs and MYBs not only regulate the key enzyme-encoding genes *PAL*, *CHS*, and *FLS* but also regulate the entire flavonoid synthesis pathway.

### Specific regulation of ROS signaling during the formation of dragon's blood

Analysis of genes involved in different signaling pathways showed that genes related to reactive oxygen species (ROS)



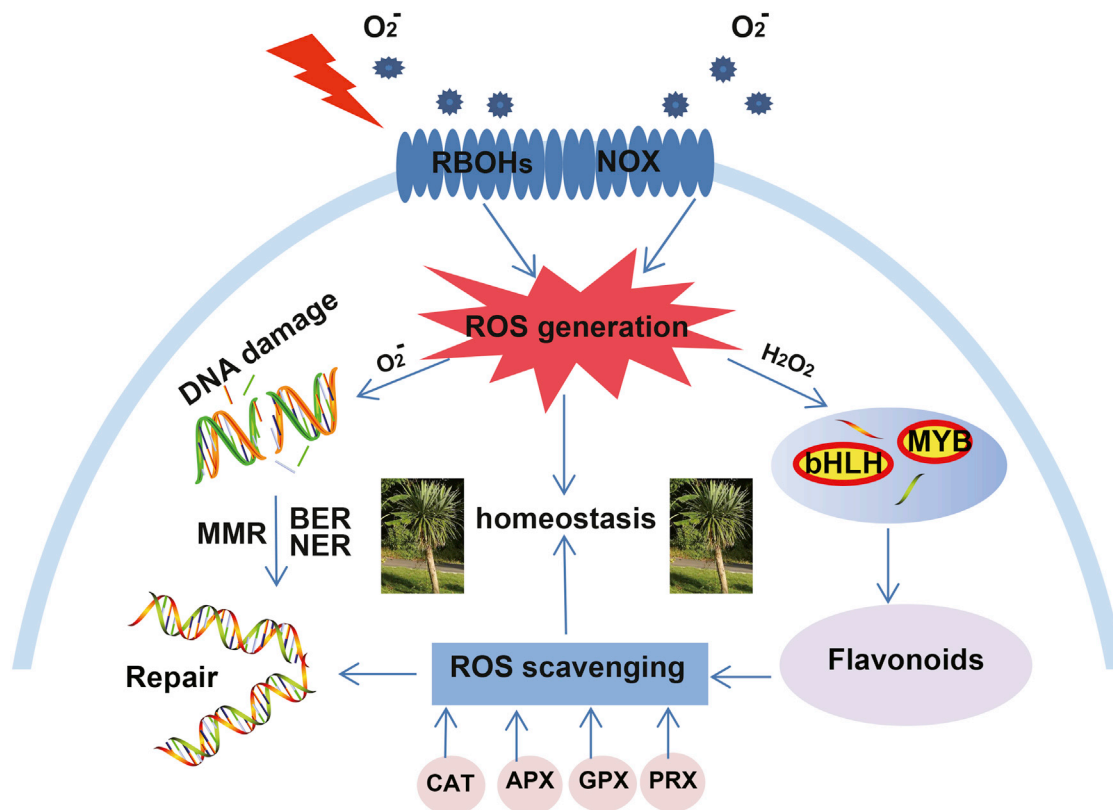


**Figure 7. A proposed model for ROS as a specific regulatory signal in the adaptation of *D. cochinchinensis*.**

An external wound leads to a burst of ROS. Excessive levels of ROS cause DNA damage. Most of the positively selected genes in the genome were enriched in DNA-repair pathways such as base excision repair, nucleotide excision repair, and mismatch repair; these processes play crucial roles in maintaining genomic integrity. ROS, as signaling molecules, also activate transcription factors, thus activating the flavonoid synthesis pathway to synthesize a large amount of flavonoids. Flavonoids are the main components of dragon's blood and act as a defensive substance to resist further damage. In turn, flavonoids, together with enzymes in the ROS scavenging system, scavenge the excess ROS that have accumulated *in vivo* to maintain homeostasis.

production and scavenging were substantially upregulated (Supplemental Figure 17). The oxidative burst is a common early event in plant defense responses, during which ROS rapidly accumulate following injury. The generation of ROS depends on NADPH oxidase and apoplastic peroxidases (Bolwell and Wojtaszek, 1997). Peroxisomes are the major sites of intracellular  $H_2O_2$  accumulation as a consequence of their oxidative metabolism (del Río et al., 2006). From the transcriptome data, we found that several enzymes, such as respiratory burst oxidase homolog, amine oxidases, NAD(P)H oxidases, and peroxidase, contributed to ROS generation and were significantly upregulated 2 h after injury (Supplemental Figure 17). Thereafter, ROS scavenging enzymes, such as superoxide dismutase, ascorbate peroxidase, glutathione peroxidase, and catalase, were also upregulated (Supplemental Figure 17). Obviously, the degree of oxidative stress is determined by the level of ROS, and the balance between ROS and antioxidants is essential if a plant is to maintain a balanced redox state.

$H_2O_2$  is the most stable type of ROS within plants. To preliminarily validate the  $H_2O_2$  response during the formation of dragon's blood, we detected the changes in  $H_2O_2$  content within stems of *D. cochinchinensis* over time after mechanical damage. The

concentration of  $H_2O_2$  increased just 1 h after mechanical damage and continued to increase to maximal levels at 6 h. After 8 h, the concentration of  $H_2O_2$  began to decrease slightly until the minimum value was reached at 5 days (Supplemental Figure 18). By contrast, other signals, such as ethylene, nitric oxide, and brassinosteroids, showed no specific changes in response to injury (Supplemental Figures 19–21). We infer that ROS act as the first sensor and represent the core signal regulator during the formation of dragon's blood (Figure 7). This is consistent with the conclusion that ROS generation represents a point at which various signaling pathways converge (Camejo et al., 2016; Sewelam et al., 2016).

## DISCUSSION

Dragon's blood is a precious traditional medicine with multiple therapeutic applications (Masaoud et al., 1995; Gupta et al., 2008; Yang and Yao, 2011; Xin et al., 2013; Fan et al., 2014; Ding et al., 2020; Madéra et al., 2020). *D. cochinchinensis* is one of the most important genuine resources of Chinese dragon's blood. Here, we constructed a high-quality reference genome for this valuable species at the chromosome level by combining PacBio sequencing and Hi-C data. The genome sequence of *Dracaena* reported herein will facilitate our

understanding of the fundamental biology of this species and provide a foundation from which to generate strategies for protection and regeneration.

*Dracaena* is world famous for its longevity (Gupta et al., 2008; Tomlinson and Huggett, 2012; Zheng et al., 2012; Madèra et al., 2018). However, the molecular mechanisms that underlie its unique biological traits remain unclear. Our analysis revealed that *D. cochinchinensis* has experienced two genome duplication events, one shared with *A. officinalis* and another that occurred independently after their divergence (Figure 2B). In addition, two LTR insertion bursts occurred recently (Figure 2C). Comparative genomic analysis revealed that expansions of *SAUR* and *cZOGT* genes are likely to be the main factors responsible for the longevity and slow growth of *D. cochinchinensis* (Figure 3). In addition, genes in the DNA repair pathway were found to be positively selected, thus contributing to genome maintenance and environmental adaptability (Supplemental Table 13).

Dragon's blood, the red resin of *Dracaena*, is a defensive substance produced by *Dracaena* when it is damaged or infected by pathogenic microorganisms (Wang, 2007; Jura et al., 2016; Ding et al., 2020; Madèra et al., 2020). Flavonoids are known to exhibit pharmacological effects and represent the main component of dragon's blood; furthermore, flavonoids are highly beneficial to *Dracaena* during growth and development. For example, flavonoids are associated with plant defense against pathogens and microbes and the absorption of free radicals and ultraviolet light (Neill and Gould, 2003; Crozier et al., 2006; Agati et al., 2009, 2011; Agati and Tattini, 2010; Landi et al., 2015). In the present study, we aimed to identify differentially expressed pathways and differential metabolites during the formation of dragon's blood. We also attempted to identify genes responsible for regulating the biosynthesis of flavonoids in *D. cochinchinensis*. We found that several secondary metabolite-related pathways, including those related to flavonoids, the terpenoid backbone, and phenylpropanoid biosynthesis, were upregulated 0–6 months after injury (Figure 5). Correspondingly, metabolomic analysis showed that the levels of flavonoid compounds increased significantly, along with those of phenylpropanoids, phenols, and phenolic acids. By contrast, the levels of coumarins, organic acids, and amine compounds were significantly reduced (Figure 4C; Supplemental Figure 13; Supplemental Table 18). Upregulated genes related to the biosynthesis of secondary metabolites included *PAL*, *CHS*, and methyltransferase; these genes are all involved in the flavonoid biosynthesis pathway. The dynamic expression profiles of genes in the flavonoid biosynthesis pathway during dragon's blood formation revealed that most of them were induced, including *CHS*, *CHI*, *F3H*, *FLS*, and *PPO*; these were only expressed at very low levels in healthy stems but were rapidly and significantly induced after injury. These changes are considered to be specifically involved in the formation of dragon's blood (Figure 6). This pattern of gene expression is essentially consistent with our results relating to differential metabolites and metabolic pathways (Figures 4C and 5). Furthermore, bHLH and MYB transcription factors were predicted to be core regulators of the flavonoid biosynthesis pathway (Supplemental Figures 14–16); these results are consistent with previous studies showing that MYB,

bHLH, and WD40 transcription factors participate in flavonoid metabolism by regulating many structural genes (Hichri et al., 2011; Schaart et al., 2013). The corresponding relationship between these transcription factors and their targets was also predicted, thus providing important clues for studying the function of these genes and their regulatory mechanisms. Further studies are now required to comprehensively elucidate the process by which the red resin is formed in *D. cochinchinensis* and thereby enable controlled and reasonable extraction of dragon's blood for commercial purposes.

To reveal the regulatory network of dragon's blood formation induced by injury, we systematically analyzed a range of signaling pathways and considered ROS to be the most crucial signal stimuli. Genes associated with ROS generation and scavenging were all upregulated after injury (Supplemental Figure 17). Moreover, the concentration of H<sub>2</sub>O<sub>2</sub> showed regular dynamic changes at different time points after injury (Supplemental Figure 18), and genes related to the main site of ROS production were also expanded (Supplemental Tables 12 and 23). *D. cochinchinensis* grows in limestone areas that are exposed to strong sunlight and high UV-B; these stimuli can cause the degradation of CP43 and CP47 and reduce photosynthetic capacity, thus leading to ROS production, DNA damage, and protein denaturation (Takshak and Agrawal, 2019). KEGG pathway analysis indicated that many of the positively selected genes were related to these deleterious processes; they participated in pathways such as base excision repair, nucleotide excision repair, mismatch repair, and DNA replication (Supplemental Table 13), implying that *D. cochinchinensis* has adapted to the environment during evolution to maintain genomic integrity. In addition, gene families involved in phenylpropanoid biosynthesis and the photosynthesis pathway were all expanded (Supplemental Tables 12 and 23). An increasing body of evidence supports the fact that flavonoids have multiple photoprotective effects (Winkel-Shirley, 2002; Agati and Tattini, 2010) and can function as ROS scavengers (Yamasaki et al., 1997; Agati et al., 2009) as well as moderators of auxin transport (Peer and Murphy, 2007). We believe there are some potential associations in *D. cochinchinensis* relating to ROS signaling, flavonoid biosynthesis, and environmental adaptability (Figure 7). This system is the result of adaptation to the environment during the process of evolution. We hypothesize that the longevity of *D. cochinchinensis* depends on its strong self-healing ability and environmental adaptability.

In summary, this study reports a genome assembly for *D. cochinchinensis* at the chromosome level, the first genome for *Dracaena* Vand. ex L. It provides a valuable genetic resource and creates significant scope for studying *Dracaena*. We revealed the genetic basis of the longevity and slow growth of *Dracaena* at the genomic level. We also provided a preliminary analysis of the molecular mechanisms associated with injury-induced flavonoid biosynthesis to form dragon's blood by performing transcriptomic and metabolomic analysis. These findings are important, as they improve our understanding of *Dracaena* adaptation, resource protection, and utilization. Further research is likely to have significant benefits for human medicine and health.

## METHODS

### Plant materials, library construction, and genome sequencing

All plant materials used in this study were 10-year-old adult *D. cochinchinensis* trees growing in the germplasm bank of *Dracaena* at the Yunnan Branch of the Institute of Medicinal Plant Development, Chinese Academy of Medical Sciences (Jing-hong City; N:22.0058°, E:100.7885°); the plants were formally identified by Professor Hai-tao Li.

Total genomic DNA was extracted from fresh young leaves using the DNeasy Plant Mini Kit (QIAGEN Bio-Tec, Hilden, Germany). The DNA was sheared by a Covaris M220 focused ultrasonicator (Covaris, Woburn, MA, USA) to create fragment sizes of 350 bp. Four types of libraries were constructed: (1) a short-read sequencing library with 350-bp insertions sequenced with the Illumina HiSeq X Ten instrument platform; (2) linked-read sequencing libraries constructed on the 10x Genomics GemCode platform and sequenced with the Illumina platform; (3) a SMRT cell library with an insert size of 20 kb for PacBio sequencing; and (4) a chromatin interaction mapping (Hi-C) library with 350-bp insertions for Illumina sequencing.

### Genome assembly and assessment of assembly quality

*De novo* assembly of PacBio single-molecule long reads from SMRT sequencing was performed using FALCON (<https://github.com/PacificBiosciences/FALCON/>) (Chin et al., 2013). BWA-MEM (Li, 2013) was used to align the 10x Genomics data to the assembly using default settings. Scaffolding was performed by fragScaff (v.1.1) with barcoded sequencing reads. These contigs were used to form super scaffolds. BWA (v.0.7.8) (Li and Durbin, 2009) software was then used to align the clean Hi-C data to the preceding assembly. According to the linkage information and restriction enzyme sites, the string graph formulation was used to construct a scaffold graph with LACHESIS (Burton et al., 2013).

### Genome annotation

Genome repeat sequences were annotated *de novo* by RepeatMasker (<http://www.repeatmasker.org>). Protein-coding genes were predicted based on the repeat-masked genome, homologous conserved proteins, and assembled transcripts. microRNA and small nuclear RNA genes were predicted by INFERNAL software using the Rfam database (detailed methods related to genome annotation are given in Supplemental Method 5).

### Gene family construction and phylogenetic analysis

Gene families were generated by OrthoMCL (v.12.0.9) (Li et al., 2003). First, nucleotide and protein data from 17 species, including *D. cochinchinensis*, *A. officinalis* (Harkess et al., 2017), *D. officinale* (Yan et al., 2015), *A. shenzhenica*, *E. guineensis*, *O. sativa* (phytozomev10), *A. comosus* (Ming et al., 2015), *M. acuminata* (D'hont et al., 2012), *A. thaliana* (phytozomev10), *P. trichocarpa* (release-32), *A. sinensis*, *H. brasiliensis*, *C. grandis*, *C. papaya* (Phytozome.ASGPBv0.4), *E. grandis*, *V. vinifera* (phytozomev10), and *A. trichopoda* (release-32) were downloaded from Ensembl (Release 70), NCBI, and <http://marinegenomics.oist.jp/gallery/>. Before running an “all against all” blastp (E value  $\leq 1E-07$ ) program, the longest transcript was selected from among the alternative splicing transcripts of each gene, and genes predicted to encode  $\leq 50$  amino acids were removed. To identify homologous gene pairs, more than 30% coverage of the aligned regions in both homologous genes was required. Finally, the alignments were clustered into gene families using OrthoMCL (v.2.0.9) (Li et al., 2003) with a 1.5 inflation index.

Protein sequences from 252 single-copy gene families were used for phylogenetic tree construction. MUSCLE (v.3.7) (Edgar, 2004) was used to generate multiple sequence alignment for protein sequences in each single-copy family with default parameters. RAxML (v.8.0.19) (Stamatakis, 2006) was used to construct the phylogenetic tree. Divergence times were estimated using MCMCTree in PAML (v.4.9) (Yang, 2007). Five calibration

points were selected and applied: *V. vinifera* and *O. sativa* (130–200 Mya) (lorizzo et al., 2016); *O. sativa* and *A. shenzhenica* (137–156 Mya) (Zhang et al., 2017a); *V. vinifera* and *C. papaya* (114–134 Mya) (Ming et al., 2008); *P. trichocarpa* and *A. thaliana* (107–109 Mya) (Tuskan et al., 2006); and *H. brasiliensis* and *P. trichocarpa* (65–86 Mya) (Tuskan et al., 2006; Tang et al., 2016).

### Expansion and contraction of gene families

Gene gain and loss in different gene families were determined using CAFÉ (v.2.2). The enriched KEGG pathways in the expanded gene families of *D. cochinchinensis* were summarized and visualized using KOBAS software.

### WGD

To investigate the genomic evolution of *D. cochinchinensis*, we identified collinearity within the *D. cochinchinensis* genome and between the *D. cochinchinensis* genome and the genomes of *A. officinalis*, *D. officinale*, and *A. shenzhenica*. We searched for putative paralogs and orthologs within and between genomes with MCScanX based on BLASTP alignment (with an E value  $\leq 1E-5$ ) for each genome pair. 4Dtv values were calculated based on each gene pair in a syntenic block, and values of all gene pairs were plotted to identify putative WGD events in *D. cochinchinensis*. We also identified different modes of gene duplication as WGDs, tandem duplicates, proximal duplicates, transposed duplicates, or dispersed duplicates using DupGen\_finder (Qiao et al., 2019) with default parameters.

### Dynamics of LTR-RTs

We investigated the dynamics of LTR-RTs in the genomes of *D. cochinchinensis*, *A. officinalis*, and *A. shenzhenica*. *De novo* detection of LTR-RTs was performed using LTRharvest (v.1.5.8) (-motif tgca -motif-mis 1) and LTRfinder (-minlenltr 100 -maxlenltr 5000 -mindistltr 1000 -maxdistltr 20000) (Ellinghaus et al., 2008). Primer-binding site motifs were annotated using LTRdigest (v.1.5.8) (Steinbiss et al., 2009), and only elements containing primer-binding site motifs were retained for further domain annotation. The domains of RTs were identified by searching against HMM profiles collated by the Gypsy Database (<http://gydb.org/>), and the internal features of LTR-RTs were annotated with LTRdigest (v.1.5.8) (Steinbiss et al., 2009). Intact LTR-RTs that contained domains (e.g., the gag domain, protease domain, reverse transcriptase domain, and integrase domain) were clustered, and those belonging to families with fewer than five members were discarded. The nucleotide divergence rate ( $\lambda$ ) was calculated from the MUSCLE alignment of the 5' and 3' LTR sequences of LTR-RTs with the EMBOSS program distmat. The insertion date (T) was computed for each LTR-RT ( $T = K/2r$ , K: genetic distance,  $K = -0.75 \ln(1 - 4\lambda/3)$ ), which was set to a substitution rate (r) of  $1.3E-08^8$  substitutions per site per year. The translated amino acid sequences were then searched for *Ty1/Copia* (PF07727) and *Ty3/Gypsy* (PF000078) domains using HMMER (v.3.1b2) (Johnson et al., 2010) (E value  $\leq 1E-5$ ). The amino acid sequences of the two superfamilies were then aligned using MAFFT (v.7.310) (Katoh and Standley, 2013), and phylogenetic trees for *Copia* and *Gypsy* LTR-RTs were constructed using FastTree (<http://www.microbesonline.org/fasttree/>).

### Detection of key candidate functional genes

We used hmmssearch (HMMER v.3.1b2) (Johnson et al., 2010) and BLASTP (E value  $\leq 1E-05$ ) (BLAST+ 2.71) (Altschul et al., 1997; Johnson et al., 2008) to identify genes involved in the biosynthesis of flavonoids based on amino acid sequences from *O. sativa* and genes involved in ROS signaling pathways based on amino acid sequences from *A. thaliana*. The candidates were further curated using the NCBI nonredundant protein database, and incorrect proteins were removed manually.

### RNA sequencing and analysis

Five tissues (root, stem, leaves, flower, and fruit) were harvested from *D. cochinchinensis*, as well as 33 cut and injury-treated stems at different

time points (0, 2, 6, 12, and 24 h, 2, 3, 4, 5, 10, 15, and 30 days, and 6 and 17 months). Three biological replicates of each tissue were collected. Raw reads from different samples were filtered to obtain high-quality clean reads following standard protocols. For gene expression analysis, clean reads were mapped to the *D. cochinchinensis* genome using TopHat (v.2.0.8) (Kim et al., 2013). Then, the read counts for each gene were normalized for downstream analysis. A gene was defined as expressed if its value of reads per kilobase per million reads mapped was  $\geq 1$  in at least one of the transcriptomes.

Differential expression analysis between a treatment sample and the control sample was performed using the DESeq R package (v.1.18.0). The resulting p values were adjusted using Benjamini and Hochberg's approach to control the false discovery rate. Genes with an adjusted p < 0.05 identified by DESeq were classified as being differentially expressed. KEGG pathway enrichment analysis of the differentially expressed genes was performed using KOBAS software (Mao et al., 2005).

#### Metabolite profiling based on ultra-high-performance liquid chromatography (LC) Q-Exactive Orbitrap mass spectrometry (MS) UHPLC-Q-Orbitrap-MS

Six healthy ~10-year-old adult trees of *D. cochinchinensis* were selected, and a 6-cm<sup>3</sup> (length: 3 cm; width: 2 cm; depth: 1 cm) wound was artificially cut using a small knife in the smooth xylem stem area of each tree. Then, 5% (v/v) benzoic acid was sprayed on the wound to prevent microbial effects (5 ml each day), and 3 months later, the xylem stem with red resin was collected from each tree. We also collected a sample of healthy xylem stem surrounding each wound. The freeze-dried samples were dissolved in 50% methanol-water (v/v) solutions at a concentration of 5 g·ml<sup>-1</sup>. The solutions were filtered and centrifuged at 13 200 × g for 10 min, and 10 μl of the resulting supernatant was directly injected into the LC-MS system.

Untargeted metabolomics was performed using a U3000 UHPLC equipped with a Q-Exactive Q-Orbitrap MS through an HESI source (Thermo Fisher Scientific, Waltham, MA, USA). A Waters Acquity UPLC HSS T<sub>3</sub> column (2.1 × 100 mm, 1.8 μm) was used for chromatographic separation with a column temperature of 35°C. The flow rate was set to 0.4 ml·min<sup>-1</sup>, and the autosampler temperature was maintained at 4°C.

The mobile A and B phases were 0.1% formic acid-water (v/v) and acetonitrile, respectively. The following elution gradient was used: 10% B in 0–3 min; 10%–22% B in 3–5 min; 22%–27% B in 5–7 min; 27%–45% B in 7–25 min; 45%–57% B in 25–35 min; 57%–100% B in 35–36 min; 100% B in 36–37 min; 100%–10% B in 37–37.5 min; and 10% B in 37.5–40 min.

The HESI source parameters were as follows: the scan mode was full-ms/dd-ms mode, and the scanning range was m/z 150–1500 at a resolution of 70 000; the spray voltage was 3.0 kV in the positive mode and 2.8 kV in the negative mode; the capillary temperature and probe heater temperature were 320°C and 350°C, respectively; the sheath gas (N<sub>2</sub>) was 35 arbitrary units, and the auxiliary gas was 10 arbitrary units (99.9% pure N<sub>2</sub>). The S-lens level value was 50 V. The normalized collision energy was 20/40/60 V. Data acquisition was performed using Xcalibur 4.1 software (Thermo Fisher Scientific).

The metabolites were identified or tentatively identified as follows: first, we used a full MS/dd-MS<sub>2</sub> (TopN) scan method that included a precursor ions list involving all of the secondary metabolites ever isolated from *Dracaena*, and the “If idle-pick others” function was used to sensitively characterize the metabolites within one injection analysis. Literature on the phytochemistry of *Dracaena* retrieved from CNKI ([www.cnki.net](http://www.cnki.net)), PubChem (<http://pubchem.ncbi.nlm.nih.gov>), Web of Science ([www.webofknowledge.com](http://www.webofknowledge.com)), ChemSpider ([www.chemspider.com](http://www.chemspider.com)), and Chemicalbook ([www.chemicalbook.com](http://www.chemicalbook.com)) was summarized (up to January 2022), and all the isolated compounds were included in the precursor ions list. Second, for compounds not annotated by the above method, we used Compound

Discoverer 3.1 (Thermo Fisher Scientific), a software tool for untargeted metabolomics, to achieve unknown identification using the following parameters: polarity, negative/positive; maximum shift, 0.2 min; mass tolerance, 5 ppm; minimum peak intensity, 100 000. The compounds were annotated with different types of databases, including m/z Cloud, ChemSpider, and the CD internal database. After data preprocessing, a peak table was generated containing m/z, retention time, and peak areas of each compound in all samples. The identification levels for all compounds were in accordance with the Metabolomics Standards Initiative (Blaženović et al., 2018).

#### Data processing of metabolomic assays

Data processing of the metabolomic assays was performed using SIEVE 2.2 (Thermo Fisher Scientific) for background subtraction and component extractions. The obtained peak list was further processed by principal component analysis and Student's t-tests to compare changes in compound composition before and after wounding stress. Principal component analysis was performed with the SIMCA-P program v.14.1 (Umetrics, Umea, Sweden). The paired-sample Student's t-tests were performed using Office Excel 2010 (Microsoft, Redmond, WA, USA), and the obtained p values were corrected using a false discovery rate (FDR) calculated in the R programming language. The null hypothesis was that the content of a compound showed no significant difference before and after the formation of dragon's blood (FDR < 0.01). SIMCA-P 14.1 was also used to transform data for orthogonal partial least squares discriminant analysis. To ensure the reliability of the data analysis, variable importance in projection values, which are the weighted values of variation obtained from orthogonal partial least squares discriminant analysis, were used as another measure to screen for differential compounds. Metabolites with a variable importance in projection >1.0 and FDR < 0.01 were chosen for further analysis of differential compounds before and after wounding stress. Multiple Experiment Viewer software (<http://mev.tm4.org/>) was used for the generation of heatmaps. Prism 6 (GraphPad, San Diego, CA, USA) was used to produce box plots and line graphs.

#### DATA AVAILABILITY

The raw genome and transcriptome sequencing data reported in this paper have been deposited in the Genome Sequence Archive (Wang et al., 2017) in the BIG Data Center, Beijing Institute of Genomics (BIG), Chinese Academy of Sciences, BioProject ID: PRJCA007701. They will be publicly accessible at <http://bigd.big.ac.cn/gsa> when the paper is accepted. The metabolome data (LC-MS datasets) will be publicly accessible at <https://ngdc.cncb.ac.cn/omix> under accession number OMIX001136-30-01 with BioProject ID (PRJCA007701).

#### SUPPLEMENTAL INFORMATION

Supplemental information is available at *Plant Communications Online*.

#### FUNDING

This work was supported by the program of the CAMS Initiative for Innovative Medicine (2021-1-I2M-032), the National Natural Science Foundation of China (82173925 and 81573525), and the National Key Research and Development Program of China (2018YFC1706401).

#### AUTHOR CONTRIBUTIONS

Y.X. and J.W. conceived and designed the project. Y.X. organized the manuscript and supervised and participated in all the related analyses. K.Z. managed the bioinformatics analyses. Z.Z. conducted metabolome analysis. Y.L. carried out the H<sub>2</sub>O<sub>2</sub> determination experiment. Y.X., Z.Z., and Y.L. contributed to sample preparation for genome and RNA sequencing. F.L., P.S., S.G., Q.W., C.Y., J.J., C.L., M.S., Z.G., C.S., H.L., Y.J., and X.G. provided constructive suggestions. All authors contributed to the writing of the paper.

#### ACKNOWLEDGMENTS

The authors declare no competing financial interests. No conflict of interest is declared.

Received: January 25, 2022  
 Revised: August 15, 2022  
 Accepted: September 29, 2022  
 Published: October 3, 2022

## REFERENCES

- Adolt, R., Habrova, H., and Madera, P.** (2012). Crown age estimation of a monocotyledonous tree species *Dracaena cinnabari* using logistic regression. *Trees (Berl.)* **26**:1287–1298. <https://doi.org/10.1007/s00468-012-0704-9>.
- Adolt, R., and Pavlis, J.** (2004). Age structure and growth of *Dracaena cinnabari* populations on Socotra. *Trees Struct. Funct.* **18**:43–53.
- Agati, G., Biricolti, S., Guidi, L., Ferrini, F., Fini, A., and Tattini, M.** (2011). The biosynthesis of flavonoids is enhanced similarly by UV radiation and root zone salinity in *L. vulgare* leaves. *J. Plant Physiol.* **168**:204–212.
- Agati, G., Stefano, G., Biricolti, S., and Tattini, M.** (2009). Mesophyll distribution of 'antioxidant' flavonoid glycosides in *Ligustrum vulgare* leaves under contrasting sunlight irradiance. *Ann. Bot.* **104**:853–861.
- Agati, G., and Tattini, M.** (2010). Multiple functional roles of flavonoids in photoprotection. *New Phytol.* **186**:786–793.
- Altschul, S.F., Madden, T.L., Schäffer, A.A., Zhang, J., Zhang, Z., Miller, W., et al.** (1997). Gapped BLAST and PSI-BLAST: a new generation of protein database search programs. *Nucleic Acids Res* **25**:3389–3402. <https://doi.org/10.1093/nar/25.17.3389>.
- Blaženović, I., Kind, T., Ji, J., and Fiehn, O.** (2018). Software tools and approaches for compound identification of LC-MS/MS data in metabolomics. *Metabolites* **8**:31.
- Bolwell, G.P., and Wojtaszek, P.** (1997). Mechanisms for the generation of reactive oxygen species in plant defence—a broad perspective. *Physiol. Mol. Plant Pathol.* **51**:347–366.
- Burton, J.N., Adey, A., Patwardhan, R.P., Qiu, R., Kitzman, J.O., and Shendure, J.** (2013). Chromosome-scale scaffolding of de novo genome assemblies based on chromatin interactions. *Nat. Biotechnol.* **31**:1119–1125.
- Cai, X.T., and Xu, Z.F.** (1979). A Study on the resource of Chinese dragon's blood. *Acta Bot. Yunnanica* **1**:1–10.
- Camejo, D., Guzmán-Cedeño, Á., and Moreno, A.** (2016). Reactive oxygen species, essential molecules, during plant-pathogen interactions. *Plant Physiol. Biochem.* **103**:10–23.
- Chin, C.S., Alexander, D.H., Marks, P., Klammer, A.A., Drake, J., Heiner, C., Clum, A., Copeland, A., Huddleston, J., Eichler, E.E., et al.** (2013). Nonhybrid, finished microbial genome assemblies from long-read SMRT sequencing data. *Nat. Methods* **10**:563–569.
- Christ, H.** (1886). *Eine Frühlingsfahrt Zu Den Canarischen Inseln* (H. Georg's Verlag).
- Crozier, A., Clifford, M.N., and Ashihara, H.** (2006). *Plant Secondary Metabolites* (Blackwell Publishers).
- D'hont, A., Denoeud, F., Aury, J.M., Baurens, F.C., Carreel, F., Garsmeur, O., Noel, B., Bocs, S., Droc, G., Rouard, M., et al.** (2012). The banana (*Musa acuminata*) genome and the evolution of monocotyledonous plants. *Nature* **488**:213–217.
- Darias, V., Bravo, L., Rabanal, R., Sanchez Mateo, C., Gonzalez Luis, R.M., and Hernandez Perez, A.M.** (1989). New contribution to the ethnopharmacological study of the Canary Islands. *J. Ethnopharmacol.* **25**:77–92.
- De Bie, T., Cristianini, N., Demuth, J.P., and Hahn, M.W.** (2006). CAFE: a computational tool for the study of gene family evolution. *Bioinformatics* **22**:1269–1271.
- del Río, L.A., Sandalio, L.M., Corpas, F.J., Palma, J.M., and Barroso, J.B.** (2006). Reactive oxygen species and reactive nitrogen species in peroxisomes. Production, scavenging, and role in cell signalling. *Plant Physiol.* **141**:330e335.
- Ding, X., Zhu, J., Wang, H., Chen, H., and Mei, W.** (2020). Dragon's blood from *Dracaena cambodiana* in China: applied history and induction techniques toward formation mechanism. *Forests* **11**:372.
- Edgar, R.C.** (2004). MUSCLE: multiple sequence alignment with high accuracy and high throughput. *Nucleic Acids Res.* **32**:1792–1797.
- Edwards, H.G.M., Farwell, D.W., and Quye, A.** (1997). 'Dragon's blood'-characterization of an ancient resin using Fourier transform Raman spectroscopy. *J. Raman Spectrosc.* **28**:243–249.
- Ellinghaus, D., Kurtz, S., and Willhoeft, U.** (2008). LTRharvest, an efficient and flexible software for de novo detection of LTR retrotransposons. *BMC Bioinform* **9**:18. <https://doi.org/10.1186/1471-2105-9-18>.
- Fan, J.Y., Tao, Y., Chui-Mei, S.T., Lin, Z., Wan-Ling, P., Ya-Zhou, Z., Zhong-Zhen, Z., and Chen, H.B.** (2014). A systematic review of the botanical, phytochemical and pharmacological profile of *Dracaena cochinchinensis*, a plant source of the ethnomedicine "Dragon's Blood". *Molecules* **19**:10650–10669.
- González, A.G., Hernández, J.C., León, F., Padrón, J.I., Estévez, F., Quintana, J., and Bermejo, J.** (2003). Steroidal saponins from the bark of *Dracaena draco* and their cytotoxic activities. *J. Nat. Prod.* **66**:793–798.
- Gupta, D., Bleakley, B., and Gupta, R.K.** (2008). Dragon's blood: botany, chemistry and therapeutic uses. *J. Ethnopharmacol.* **115**:361–380.
- Hao, Q., Saito, Y., Matsuo, Y., Li, H.Z., and Tanaka, T.** (2015). Chalcone-stilbene conjugates and oligomeric flavonoids from Chinese dragon's blood produced from *Dracaena cochinchinensis*. *Phytochemistry* **119**:76–82.
- Harkess, A., Zhou, J., Xu, C., Bowers, J.E., Van der Hulst, R., Ayyampalayam, S., Mercati, F., Riccardi, P., McKain, M.R., Kakrana, A., et al.** (2017). The asparagus genome sheds light on the origin and evolution of a young Y chromosome. *Nat. Commun.* **8**:1279.
- Hernández, J.C., León, F., Quintana, J., Estévez, F., and Bermejo, J.** (2004). Icogenin, a new cytotoxic steroidal saponin isolated from *Dracaena draco*. *Bioorg. Med. Chem.* **12**:4423–4429.
- Hichri, I., Barrieu, F., Bogs, J., Kappel, C., Delrot, S., and Lauvergeat, V.** (2011). Recent advances in the transcriptional regulation of the flavonoid biosynthetic pathway. *J. Exp. Bot.* **62**:2465–2483.
- Humboldt, A.V.** (1814). *Relation Historique Du Voyage Aux Régions Équinoxiales Du Nouveau Continent*.
- Hubáľková, I., Madera, P., and Volařík, D.** (2015). Growth dynamics of *Dracaena cinnabari* under controlled conditions as the most effective way to protect endangered species. *Saudi J. Biol. Sci.* **24**:1445–1452.
- Iorizzo, M., Ellison, S., Senalik, D., Zeng, P., Satapoomin, P., Huang, J., et al.** (2016). A high-quality carrot genome assembly provides new insights into carotenoid accumulation and asterid genome evolution. *Nat. Genet.* **48**:657–666.
- IUCN Red List.** (2017). IUCN Red List of Threatened Species Version. <http://www.iucnredlist.org>.
- Johnson, L.S., Eddy, S.R., and Portugaly, E.** (2010). Hidden Markov model speed heuristic and iterative HMM search procedure. *BMC Bioinformatics* **11**:431.
- Johnson, S.A., Dubeau, L., and Johnson, D.L.** (2008). Enhanced RNA polymerase III-dependent transcription is required for oncogenic transformation. *J. Biol. Chem.* **283**:19184–19191.
- Jura Morawiec, J.** (2019). Rhythmic growth and age estimation of aerial roots in *Dracaena draco* (Asparagaceae). *Trees* **33**:1513–1518.
- Jura-Morawiec, J., Tulik, M., and Tulik, M.** (2016). Dragon's blood secretion and its ecological significance. *Chemoecology* **26**:101–105.

- Kamel, M., Ghazaly, U.M., and Callmänder, M.W. (2018). Conservation status of the endangered Nubian dragon tree *Dracaena ombet* in Gebel Elba national park. Egypt. Oryx **49**:704–709.
- Kant, S., Bi, Y.M., Zhu, T., and Rothstein, S.J. (2009). SAUR39, a small auxin-up RNA gene, act as a negative regulator of auxin synthesis and transport in rice. Plant Physiol. **151**:691–701.
- Katoh, K., and Standley, D.M. (2013). MAFFT multiple sequence alignment software version 7: improvements in performance and usability. Mol. Biol. Evol. **30**:772–780.
- Kim, D., Perteza, G., Trapnell, C., Pimentel, H., Kelley, R., and Salzberg, S.L. (2013). TopHat2: accurate alignment of transcriptomes in the presence of insertions, deletions and gene fusions. Genome Biol. **14**:R36.
- Kim, S., Park, M., Yeom, S.I., Kim, Y.M., Lee, J.M., Lee, H.A., Seo, E., Choi, J., Cheong, K., Kim, K.T., et al. (2014). Genome sequence of the hot pepper provides insights into the evolution of pungency in Capsicum species. Nat. Genet. **46**:270–278.
- Kudo, T., Makita, N., Kojima, M., Tokunaga, H., and Sakakibara, H. (2012). Cytokinin activity of cis-zeatin and phenotypic alterations induced by overexpression of putative cis-zeatin-O-glucosyltransferase in rice. Plant Physiol. **160**:319–331.
- Landi, M., Tattini, M., and Gould, K.S. (2015). Multiple functional roles of anthocyanins in plant-environment interactions. Environ. Exp. Bot. **119**:4–17.
- Lengálová, K., Kalivodová, H., Habrová, H., Maděra, P., Tesfamariam, B., and Šenfeldr, M. (2020). First age-estimation model for dracaena ombet and dracaena draco subsp. Forests **11**:264. <https://doi.org/10.3390/f11030264>.
- Li, H. (2013). Aligning sequence reads, clone sequences and assembly contigs with BWA-MEM. Preprint at arXiv. <https://doi.org/10.48550/arXiv.1303.3997>.
- Li, H., and Durbin, R. (2009). Fast and accurate short read alignment with Burrows-Wheeler transform. Bioinformatics **25**:1754–1760.
- Li, L., Stoeckert, C.J., Jr., and Roos, D.S. (2003). OrthoMCL: identification of ortholog groups for eukaryotic genomes. Genome Res **13**:2178–2189.
- Li, S.F., Wang, J., Dong, R., Zhu, H.W., Lan, L.N., Zhang, Y.L., Li, N., Deng, C.L., and Gao, W.J. (2020). Chromosome-level genome assembly, annotation and evolutionary analysis of the ornamental plant *Asparagus setaceus*. Hortic. Res. **7**:48.
- Luo, Y., Wang, H., Zhao, Y.X., Zeng, Y.B., Shen, H.Y., Dai, H.F., and Mei, W.L. (2011). Cytotoxic and antibacterial flavonoids from dragon's blood of *Dracaena cambodiana*. Planta Med. **77**:2053–2056.
- Maděra, P., Forrest, A., Hanáček, P., Vahalík, P., Gebauer, R., Plichta, R., Jupa, R., Van Rensburg, J.J., Morris, M., Nadezhdina, N., et al. (2020). What we know and what we do not know about dragon trees? Forests **11**:236.
- Maděra, P., Habrová, H., Šenfeldr, M., Kholová, I., Lvončík, S., Ehrenbergerová, L., Roth, M., Nadezhdina, N., Némec, P., Rosenthal, J., et al. (2018). Growth dynamics of endemic *Dracaena cinnabari* Balf. f. of Socotra Island suggest essential elements for a conservation strategy. Biologia **74**:339–349. <https://doi.org/10.2478/s11756-018-0152-0>.
- Mägdefrau, K. (1975). Das alter der drachenbäume auf Tenerife. Flora **164**:347–357.
- Mao, X., Cai, T., Olyarchuk, J.G., and Wei, L. (2005). Automated genome annotation and pathway identification using the KEGG Orthology (KO) as a controlled vocabulary. Bioinformatics **21**:3787–3793.
- Masaoud, M., Schmidt, J., and Adam, G. (1995). Sterols and triterpenoids from *Dracaena cinnabari*. Phytochemistry **38**:795–796.
- Mimaki, Y., Kuroda, M., Ide, A., Kameyama, A., Yokosuka, A., and Sashida, Y. (1999). Steroidal saponins from the aerial parts of *Dracaena draco* and their cytostatic activity on HL-60 cells. Phytochemistry **50**:805–813.
- Ming, R., VanBuren, R., Wai, C.M., Tang, H., Schatz, M.C., Bowers, J.E., et al. (2015). The pineapple genome and the evolution of CAM photosynthesis. Nat. Genet. **47**:1435–1442.
- Neill, S.O., and Gould, K.S. (2003). Anthocyanins in leaves: light attenuators or antioxidants. Funct. Plant Biol. **30**:865–873.
- Nisa, M.U., Huang, Y., Benhamed, M., and Raynaud, C. (2019). The plant DNA damage response: signaling pathways leading to growth inhibition and putative role in response to stress conditions. Front. Plant Sci. **10**:653.
- Pang, D.R., Su, X.Q., Zhu, Z.X., Sun, J., Li, Y.T., Song, Y.L., Zhao, Y.F., Tu, P.F., Zheng, J., and Li, J. (2016). Flavonoid dimers from the total phenolic extract of Chinese dragon's blood, the red resin of *Dracaena cochinchinensis*. Fitoterapia **115**:135–141.
- Peer, W.A., and Murphy, A.S. (2007). Flavonoids and auxin transport: modulators or regulators? Trends Plant Sci. **12**:556–563.
- Pütter, A. (1925). Altersbestimmung an drachenbäumen von Tenerife. Sitz. Heidelb. Akad. Wissenschaften. Math.Nat. Kl. **12**:12–18.
- Qiao, X., Li, Q., Yin, H., Qi, K., Li, L., Wang, R., Zhang, S., and Paterson, A.H. (2019). Gene duplication and evolution in recurring polyploidization diploidization cycles in plants. Genome Biol. **20**:38.
- Ren, H., and Gray, W.M. (2015). SAUR proteins as effectors of hormonal and environmental signals in plant growth. Mol. Plant **8**:1153–1164.
- Pineda Rodo, A., Brugièrè, N., Vankova, R., Malbeck, J., Olson, J.M., Haines, S.C., Martin, R.C., Habben, J.E., Mok, D.W.S., and Mok, M.C. (2008). Over-expression of a zeatin O-glucosylation gene in maize leads to growth retardation and tasselseed formation. J. Exp. Bot. **59**:2673–2686.
- Schaart, J.G., Dubos, C., Romero De La Fuente, I., van Houwelingen, A.M.M.L., de Vos, R.C.H., Jonker, H.H., Xu, W., Routaboul, J.M., Lepiniec, L., and Bovy, A.G. (2013). Identification and characterization of MYB-bHLH-WD40 regulatory complexes controlling proanthocyanidin biosynthesis in strawberry (*Fragaria x ananassa*) fruits. New Phytol. **197**:454–467.
- Schuch, A.P., Moreno, N.C., Schuch, N.J., Menck, C.F.M., and Garcia, C.C.M. (2017). Sunlight damage to cellular DNA: focus on oxidatively generated lesions. Free Radic. Biol. Med. **107**:110–124.
- Schenck, H. (1907). Beiträge Zur Kenntnis Der Vegetation Der Canarischen Inseln; Wissenschaftliche Ergebnisse der Deutschen Tiefsee-Expedition auf dem Dampfer "Valdivia"2 (Fischer), pp. 225–406.
- Sewelam, N., Kazan, K., and Schenk, P.M. (2016). Global plant stress signaling: reactive oxygen species at the cross-road. Front. Plant Sci. **7**:187.
- Simão, F.A., Waterhouse, R.M., Ioannidis, P., Kriventseva, E.V., and Zdobnov, E.M. (2015). BUSCO: assessing genome assembly and annotation completeness with single-copy orthologs. Bioinformatics **31**:3210–3212.
- Singh, R., Ong-Abdullah, M., Low, E.T., Manaf, M.A., Rosli, R., Nookiah, R., et al. (2013). Oil palm genome sequence reveals divergence of interfertile species in Old and New worlds. Nature **500**:335–339.
- Stamatakis, A. (2006). RAxML-VI-HPC: maximum likelihood-based phylogenetic analyses with thousands of taxa and mixed models. Bioinformatics **22**:2688–2690.
- Steinbiss, S., Willhoeft, U., Gremme, G., and Kurtz, S. (2009). Fine-grained annotation and classification of de novo predicted LTR retrotransposons. Nucleic Acids Res **37**:7002–7013.

- Stortenbeker, N., and Bemer, M. (2019). The SAUR gene family: the plant's toolbox for adaptation of growth and development. *J. Exp. Bot.* **70**:17–27.
- Sun, J., Liu, J.N., Fan, B., Chen, X.N., Pang, D.R., Zheng, J., Zhang, Q., Zhao, Y.F., Xiao, W., Tu, P.F., et al. (2019). Phenolic constituents, pharmacological activities, quality control, and metabolism of *Dracaena* species: a review. *J. Ethnopharmacol.* **244**:112138.
- Symon, D.E. (1974). The growth of *Dracaena draco*—dragon's blood tree. *Journal of the Arnold Arboretum.* **55**:51–58.
- Takshak, S., and Agrawal, S.B. (2019). Defense potential of secondary metabolites in medicinal plants under UV-B stress. *J. Photochem. Photobiol., B* **193**:51–88.
- Tang, C., Yang, M., Fang, Y., Luo, Y., Gao, S., Xiao, X., An, Z., Zhou, B., Zhang, B., Tan, X., et al. (2016). The rubber tree genome reveals new insights into rubber production and species adaptation. *Native Plants* **2**:16073–16110.
- Teh, B.T., Lim, K., Yong, C.H., Ng, C.C.Y., Rao, S.R., Rajasegaran, V., Lim, W.K., Ong, C.K., Chan, K., Cheng, V.K.Y., et al. (2017). The draft genome of tropical fruit durian (*Durio zibethinus*). *Nat. Genet.* **49**:1633–1641.
- Teng, Z., Zhang, M., Meng, S., Dai, R., Meng, W., Deng, Y., and Huang, L. (2015). A comparative study on volatile metabolites profile of *Dracaena cochinchinensis* (Lour.) S.C.Chen xylem with and without resin using GC-MS. *Biomed. Chromatogr.* **29**:1744–1749.
- Tomlinson, P.B., and Huggett, B.A. (2012). Cell longevity and sustained primary growth in palm stems. *Am. J. Bot.* **99**:1891–1902.
- Tuskan, G.A., Difazio, S., Jansson, S., Bohlmann, J., Grigoriev, I., Hellsten, U., Putnam, N., Ralph, S., Rombauts, S., Salamov, A., et al. (2006). The genome of black cottonwood, *Populus trichocarpa* (Torr. & Gray). *Science* **313**:1596–1604.
- Vaničková, L., Pompeiano, A., Maděra, P., Massad, T.J., and Vahalík, P. (2020). Terpenoid profiles of resin in the genus *Dracaena* are species specific. *Phytochemistry* **170**:112197.
- Wang, X.H. (2007). Flavones formed from xylem stem of *Dracaena cochinchinensis* by co-culture of fungus strain and bacteria strain. *Nat. Pro. Res. Dev.* **19**:11–15.
- Wang, X.H., Gong, M., Tang, L., Zheng, S., Lou, J.D., Ou, L., Gomes-Laranjo, J., and Zhang, C. (2013). Gomes-Laranjo J; Zhang C. Cloning, bioinformatics and the enzyme activity analyses of a phenylalanine ammonia-lyase gene involved in dragon's blood biosynthesis in *Dracaena cambodiana*. *Mol. Biol. Rep.* **40**:97–107.
- Wang, X.H., Zhang, C., Yang, L.-L., and Gomes-Laranjo, J. (2011). Production of dragon's blood in *Dracaena cochinchinensis* plants by inoculation of *Fusarium proliferatum*. *Plant Sci.* **180**:292–299.
- Wang, Y., Song, F., Zhu, J., Zhang, S., Yang, Y., Chen, T., Tang, B., Dong, L., Ding, N., Zhang, Q., et al. (2017). GSA: genome sequence archive. *Genom. Dev. Reprod. Biol.* **15**:14–18.
- Winkel-Shirley, B. (2002). Biosynthesis of flavonoids and effects of stress. *Curr. Opin. Plant Biol.* **5**:218–223.
- Xin, N., Yang, F.J., Li, Y., Li, Y.J., Dai, R.J., Meng, W.W., Chen, Y., and Deng, Y.L. (2013). Dragon's blood dropping pills have protective effects on focal cerebral ischemia rats model. *Phytomedicine* **21**:68–74.
- Yamasaki, H., Sakihama, Y., and Ikehara, N. (1997). Flavonoid-peroxidase reaction as detoxification mechanism of plant cells against H<sub>2</sub>O<sub>2</sub>. *Plant Physiology* **115**:1405–1412.
- Yan, L., Wang, X., Liu, H., Tian, Y., Lian, J., Yang, R., Hao, S., Wang, X., Yang, S., Li, Q., et al. (2015). The genome of *Dendrobium officinale* illuminates the biology of the important traditional Chinese orchid herb. *Mol. Plant* **8**:922–934.
- Yang, X., and Yao, L. (2011). Pharmacological action and clinical experience of dragon's blood. *Heilongjiang Medicine Journal* **24**:265–266.
- Yang, Z. (2007). PAML 4: phylogenetic analysis by maximum likelihood. *Mol. Biol. Evol.* **24**:1586–1591.
- Zhang, G.Q., Liu, K.W., Li, Z., Lohaus, R., Hsiao, Y.Y., Niu, S.C., Wang, J.Y., Lin, Y.C., Xu, Q., Chen, L.J., et al. (2017a). The *Apostasia* genome and the evolution of orchids. *Nature* **549**:379–383.
- Zhang, L., Li, X., Ma, B., Gao, Q., Du, H., Han, Y., Li, Y., Cao, Y., Qi, M., Zhu, Y., et al. (2017b). The artary buckwheat genome provides insights into rutin biosynthesis and abiotic stress tolerance. *Mol. Plant* **10**:1224–1237.
- Zheng, D.J., Xie, L.S., Wang, Y., Zhang, Z.L., and Zhang, W. (2009). Research advances in dragon's blood plants in China. *Chin. Wild Plant Res.* **28**:15–20.
- Zheng, D.J., Xie, L.S., Zhu, J.H., and Zhang, Z.L. (2012). Low genetic diversity and local adaptive divergence of *Dracaena cambodiana* (Liliaceae) populations associated with historical population bottlenecks and natural selection: an endangered long-lived tree endemic to Hainan Island, China. *Plant Biol.* **14**:828–838.
- Zheng, Q.A., Zhang, Y.J., and Yang, C.R. (2006). A new meta-homoisoflavane from the fresh stems of *dracaena cochinchinensis*. *J. Asian Nat. Prod. Res.* **8**:571–577.